

DFT Study of Nitrogen-Substituted FAU: Effects of Ion Exchange and Aluminum Content on Base Strength

Vishal Agarwal,[†] W. Curtis Conner, Jr.,[†] and Scott M. Auerbach^{*,†,‡}

Department of Chemical Engineering, University of Massachusetts, Amherst, Massachusetts 01003, United States, and Department of Chemistry, University of Massachusetts, Amherst, Massachusetts 01003, United States

Received: July 26, 2010; Revised Manuscript Received: October 15, 2010

We have studied base strengths of nitrogen-substituted (nitrided) zeolites with faujasite (FAU) structure by calculating sorption energies of probe molecules (BF₃ and BH₃) using density functional theory with mixed basis sets applied to embedded clusters. BH₃ was found to be a better probe of base strength because it does not introduce competing metal–fluorine interactions that obfuscate trends. In all cases, the base strengths of nitrided zeolites (denoted M–N–Y) were found to exceed those of the corresponding standard M–Y zeolites, where M = Li, Na, K, Rb, or Cs charge-compensating cations. We have found that for a particular Si:Al ratio, BH₃ sorption energies vary in the order Li < Na < K ~ Rb ~ Cs. Sorption energy and hence base strength was found to decrease with increasing Si:Al ratio from 1 to 3 beyond which the base strength was found to increase again. The initial regime (1 < Si:Al < 3) is consistent with the prevailing understanding that the base strength increases with Al content, while the latter regime (Si:Al > 3) involves the surprising prediction that the base strength can be relatively high for the more stable, high-silica zeolites. In particular, we found the sorption energy in Na–N–Y (Si:Al = 11) to be nearly equal to that in (Si:Al = 1). Taken together, these results suggest that K–N–Y (Si:Al = 11) optimizes the balance of activity, stability, and cost.

1. Introduction

Zeolites are microporous crystalline materials composed of TO₄ (T = Si, Al) tetrahedra as primary units joined via oxygens to give cage-like structures.¹ Acidic zeolite catalysts have long been the backbone of the petroleum industry because of their high surface area, large adsorption capacities, and shape-selective properties. All these properties make them ideal candidates for biofuel production catalysts. However, biomass-derived feedstocks contain heavily oxygenated compounds suggesting the development of shape-selective basic catalysts, which can activate organic oxygenates by forming anionic intermediates (cf. aldol condensation²). Having a strong shape-selective solid base catalyst will also be desirable in other industries such as the fine-chemical, pharmaceutical, and food industries.^{3–5} Classes of zeolites that have base character include ion-exchanged zeolites,^{3,5} zeolites with grafted organic bases,^{3,5} nitrided zeolites,⁶ and other classes such as nickel phosphate VSB-5.⁷ We recently showed that nitridation, replacing zeolite bridging oxygens with isoelectronic amine groups (–NH–), can nearly double base strength in zeolites.⁸ A variety of studies have demonstrated the use of nitrogen-substituted zeolites as base catalysts.^{9,10} However, there has been no systematic study of base strength versus aluminum content or alkali cation in these systems. In this article, we report density functional theory calculations of adsorption energies for probe molecules on embedded zeolite clusters to reveal basicity trends in nitrogen-substituted zeolites.

Nitrided zeolites have been under study for over 40 years¹¹ since the initial report by Kerr and Shipman in 1968.⁶ Although

recent work on nitrided zeolites has revealed interesting base catalytic activities,^{9,10} the structures of nitrided zeolites and their active sites have remained only ambiguously identified.^{6,9,10,12–19} By combining ²⁹Si solid-state NMR and quantum calculations of chemical shifts, we have shown that nitridation in high-silica H–Y (Si:Al = 15) is consistent with an intact zeolite framework and occurs first at Brønsted sites (Si–OH–Al) and subsequently at siliceous sites (Si–O–Si).^{12,15,16} The story is qualitatively similar for nitridation of Na–Y (Si:Al = 2.4), although the diversity of nitrided sites in Na–Y is much higher because of the higher Al content.^{12,15,16} Furthermore, through a combination of X-ray diffraction, ²⁹Si solid-state NMR, and high-resolution adsorption studies, we have recently reported an optimal synthesis approach for nitrided zeolites emphasizing the importance of high ammonia flow rates during heating and reacting steps.^{12,15,16} Finally, density functional theory (DFT) calculations of the nitridation mechanisms in H–Y and silicalite zeolites²⁰ have been used to predict that nitrided zeolites remain stable at high temperatures even at saturation water loadings.²¹ The question still remains how the Si:Al ratio and the nature of the charge-compensating cation impact strengths of basic sites in nitrided zeolites.

A conventional wisdom in zeolite science suggests that increasing aluminum content (decreasing the Si:Al ratio) increases zeolite base strength because isomorphic substitution of aluminum for silicon increases framework negative charge hence facilitating Lewis and Brønsted base activity through increased oxygen charge density. Various experimental studies support this notion;^{22–29} however, most of these studies have been performed on FAU-type zeolites of standard X (Si:Al = 1.2) and Y (Si:Al = 2.4) compositions. Zeolites with higher Si:Al ratios have been studied by Barthomeuf²³ and Okamoto et al.,³⁰ however, they studied zeolites with different framework structures making comparisons with X and Y zeolites inap-

* To whom correspondence should be addressed. Phone: +1-413-545-1240; fax: +1-413-545-4490; e-mail: auerbach@chem.umass.edu.

[†] Department of Chemical Engineering.

[‡] Department of Chemistry.

appropriate. As such, it is not clear whether this trend continues for zeolites with Si:Al ratios much above 2.4. This is an important question because decreasing the aluminum content of zeolites (increasing Si:Al ratio) makes them more stable to the kinds of hydrothermal treatments used to regenerate catalysts. Our calculations thus serve as a guide for balancing material stability and catalytic activity. A challenge in implementing such calculations is dealing with long-range aluminum/cation distributions, which we handle using embedded clusters within the ONIOM formulation.³¹

The strength of basic sites also depends on the nature of the charge-compensating cation.²² For standard zeolites with alkali cations, base strength has been shown to increase in the order of $\text{Li} < \text{Na} < \text{K} < \text{Rb} < \text{Cs}$ ^{22–24,32} suggesting that ion exchange of nitrated zeolites (or nitridation of ion-exchanged zeolites) should produce the strongest possible basic sites. The expense of ion exchange warrants the question of how much base strength is gained by such a process. We investigate this below by calculating energies of embedded clusters using atomic basis sets such as the split-valence, triple- ζ basis set 6-311G(d,p).³³ This basis set is, however, unavailable for heavier elements such as Rb and Cs forcing a mixed basis set approach as we describe below.

Various methods are described in the literature for characterizing the basicity of zeolites. Experimental methods include the use of probe molecules such as pyrrole,^{23,25–27} chloroform,^{28,29} and but-1-yne³⁴ along with techniques such as X-ray photoelectron spectroscopy (XPS)^{25,26,29} and Fourier transform infrared (FTIR).^{23,27,28,34} Theoretical methods include analyzing charge densities using the electronegativity equalization method (EEM)³⁵ and the molecular electrostatic potential (MEP) method³² as well as the use of acidic probe molecules such as BF_3 .⁸ In our initial study on nitrated zeolites, we quantified base strength by computing adsorption energies of BF_3 in sodalite zeolites with Si–O–Si and Si–NH–Si sites finding -0.5 and -0.8 eV, respectively.⁸ For consistency, we continue below with BF_3 as a probe molecule for studying base strengths in various standard and nitrated FAU-type zeolites. However, we find below that BH_3 is a better probe of base strength because trends in adsorption energy are not obscured by competing metal–fluorine interactions. We find below that nitridation increases base strengths for all zeolites studied, but surprisingly, we also find a nonmonotonic trend in base strength versus Al content with high-silica Na–Y showing remarkably strong base sites.

The remainder of this article is organized as follows: in section 2, we describe the zeolites studied and detail the computational methods of the ONIOM calculations; in section 3, we discuss the resulting adsorption energies using BF_3 and BH_3 as probe molecules; and in section 4, we offer concluding remarks.

2. Methods

We have studied various FAU-type zeolites by calculating BH_3 and BF_3 (generally BX_3) sorption energies to gauge zeolite base strength. To determine the role of aluminum content, we have studied standard and nitrated FAU-type zeolites with silicon-to-aluminum ratios (Si:Al) of 1, 3, 5, and 11 all with Na as the charge-compensating cation. The material with Si:Al = 1 is commonly referred to as Na-LSX (low silica X), while those with Si:Al > 1.5 are denoted Na–Y zeolites. For notational convenience, we refer to all these standard and nitrated zeolites as Na–Y and Na–N–Y, respectively. To investigate the effect of changing the charge-compensating cation, we have studied

standard zeolites M–Y (Si:Al = 11) and nitrated analogues M–N–Y (Si:Al = 11) with alkali metals $M = \text{Li}, \text{Na}, \text{K}, \text{Rb},$ and Cs .

Base strength was gauged by the magnitude of sorption energies calculated according to

$$\Delta V_{\text{ads}} = V_{\text{ZG}} - V_{\text{Z}} - V_{\text{G}} \quad (1)$$

where V_i is the optimized electronic energy of zeolite-guest (ZG), zeolite (Z), and guest (G). Assuming that the zeolite, guest, and zeolite–guest complex act as multidimensional harmonic oscillators, the molar internal energy of adsorption at absolute temperature T is given by $\Delta U_{\text{ads}} = \Delta V_{\text{ads}} + 3RT$ where the second term ($3RT$) is the average harmonic potential energy of hindered translations and rotations for the guest sorbed in the zeolite. This harmonic approximation is good because BX_3 sorption produces relatively tightly bound zeolite– BX_3 structures because of the strong Lewis acidity of BH_3 and BF_3 . Furthermore, assuming that the external BX_3 gas phase is ideal, the molar enthalpy of adsorption is given by $\Delta H_{\text{ads}} = \Delta U_{\text{ads}} = \Delta V_{\text{ads}} + 2RT$; this ideal gas approximation is also supported by the large sorption energies reported below. Thus, calculating ΔH_{ads} reveals trends in sorption heats, and hence base strengths, for the zeolites studied herein. By convention, we report all sorption energies below as positive quantities.

The acid–base interaction that controls sorption energies in these systems is of a strongly chemical nature requiring quantum calculations to capture trends in base strength. All calculations in this work were performed using a finite zeolite cluster model. Although this approach lacks true long-range forces, it captures local interactions quite well, such as acid–base binding in silica-based materials. Indeed, in previously published cluster calculations, we computed the sorption energy of ammonia in H–Y as 111 kJ/mol,²⁰ which compares well with the range of experimental values 100–130 kJ/mol.^{36–38} The calculations below used the same total system cluster size as in our previous work.²⁰

The FAU zeolite framework topology exhibits four crystallographically distinct oxygens³⁹ of which O(1) and O(4) are the most accessible, being in the window separating adjacent FAU supercages, making these oxygen sites relevant for catalysis. Moreover, previous simulations have found that O(1) and O(4) are the most basic oxygens in FAU-type zeolites.³⁵ In this work, we have performed sorption studies on the O(1) oxygen site, while for nitrated zeolites, we have modeled sorption at the nitrated O(1) site. In our previous work,²⁰ we found substantially similar nitridation energies at O(1) and O(4) in HY indicating little sensitivity to nitridation site. This indicates that other clusters of the same size, but centered on a different oxygen in the FAU structure, will give substantially similar results.

We have used the embedded cluster approach via two-layer ONIOM^{40–42} for computing optimized geometries and energies in this work. Here, we describe the construction of clusters followed by details of the ONIOM calculations. BH_3 and BF_3 adsorption was studied on the same clusters. We built 92T clusters centered at O(1) containing 92 total silicon and aluminum (tetrahedral or T) atoms consistent with our previous cluster calculations.²⁰ All clusters were terminated with oxygen atoms fixed at their crystallographically determined locations (vide infra). At the core of each 92T cluster, a 12T quantum cluster was extracted, and its dangling bonds were passivated as discussed below. This quantum cluster size has proven sufficient to converge acid–base energetics in zeolites.^{20,31} To study the effect of ion exchange, we built 12T quantum clusters

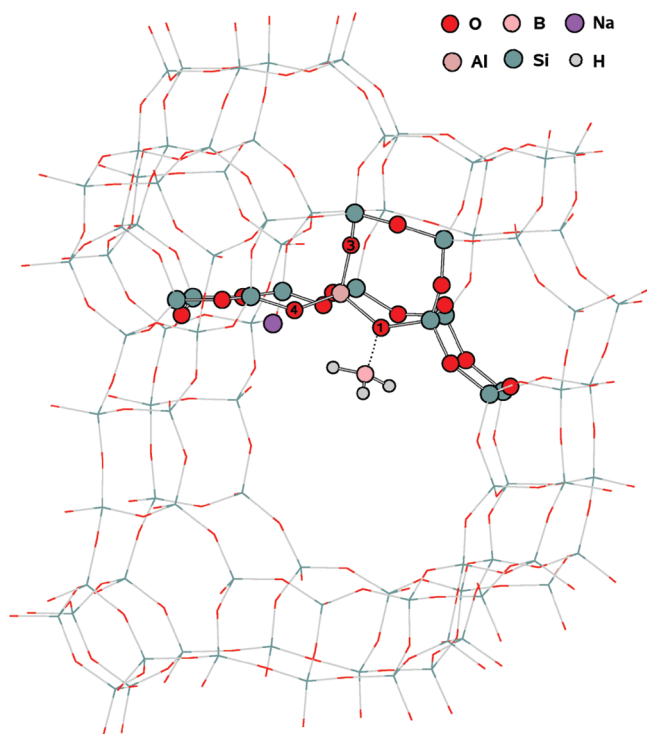


Figure 1. Structure of BH_3 in 12T quantum cluster embedded in 92T cluster model of Na-Y.

with an isolated aluminum substitution adjacent to O(1) balanced by one alkali metal giving a Si:Al ratio of 11 in the quantum cluster. The outside layer for this system was taken as purely siliceous from the X-ray crystal structure of zero-defect dealuminated Y zeolite³⁹ (ZDDAY or siliceous FAU, fcc with a 24.3 Å lattice parameter). As such, this represents an isolated basic site with various charge-compensating cations, which were initialized near site II close to the supercage six-ring.^{43,44}

To study the effect on basicity of varying aluminum content, we built 12T quantum clusters with 1, 2, 3, and 6 aluminum substitutions balanced by equal numbers of Na atoms giving Si:Al ratios of 11, 5, 3, and 1, respectively. Each outside layer was built to match the Si:Al ratio of the inside quantum layer. This was achieved by using forcefield-based simulations to generate initial conditions for ONIOM optimizations. For Si:Al = 1, we began with the alternating aluminum distribution dictated by Löwenstein's rule¹ and optimized the Na distribution using the forcefield of Jaramillo and Auerbach.⁴⁴ From this optimized 192T unit cell of Na-LSX (24.9 Å lattice parameter), we extracted a 92T total cluster, and from this cluster, we extracted a 12T quantum cluster, and both were centered at O(1). For each higher Si:Al ratio, we began with the Na-LSX structure and converted the appropriate number of aluminums back to silicons to achieve the target Si:Al ratio. Each aluminum switch was chosen at random, and the closest Na atom was deleted. Special care was taken to maintain a homogeneous distribution of Na atoms for each Si:Al ratio. As above, 92T total system clusters centered at O(1) were then extracted, and from these, 12T quantum clusters were built. This approach does not guarantee that the resulting 12T quantum cluster contains the desired number of Al/Na atoms; several iterations were performed until acceptable initial structures were obtained.

In two-layer ONIOM,^{40–42} the 92T total system cluster is denoted "S" while the passivated 12T quantum cluster is denoted "C." A snapshot of the cluster NaY with adsorbed BH_3 is shown in Figure 1. No electrostatic interaction between the quantum

TABLE 1: Test of Mixed Basis Set Using BF_3 Sorption Energies (Si:Al = 11)

structure	sorption energy (kJ/mol) ^a	difference (kJ/mol)	% difference
Li-Y	-70.9 (-73.9)	3.0	4.2
Li-N-Y	-115.2 (-119.0)	3.8	3.3
Na-Y	-77.9 (-79.7)	1.8	2.3
Na-N-Y	-121.4 (-123.6)	2.2	1.8
K-Y	-90.3 (-90.9)	0.6	0.7
K-N-Y	-135.9 (-136.6)	0.7	0.5

^a Sorption energies were calculated at B3LYP level of theory in quantum layer and UFF for the total system. SDD basis set was used for alkali atoms, and 6-311G(d,p) was used for all other atoms. The values in parentheses are those from using 6-311G(d,p) for all atoms.

cluster and the rest of the total system was considered, that is, the calculations were performed using mechanical embedding but not electronic embedding. All 12T quantum clusters consisted of one six-ring and three four-rings as shown in Figure 1; these were terminated via Si-H and Al-H groups with hydrogen atoms placed along Si-O or Al-O vectors for each omitted oxygen. Although terminating with Si-OH and Al-OH groups is preferable, the Si-H/Al-H terminations were used to mitigate the computational expense of including (as many as six) Na atoms in the quantum clusters. Nonetheless, we have found that such terminations are acceptable for modeling acid-base chemistry with such large (12T) quantum clusters.^{20,31}

The total system electronic energy is approximated within ONIOM from three independent calculations according to⁴⁵

$$E_{\text{ONIOM}} = E_{\text{hi}}(\text{C}) + [E_{10}(\text{S}) - E_{10}(\text{C})] \quad (2)$$

where subscripts "hi" and "lo" represent high and low levels of theory, respectively. For the high level of theory, we used the B3LYP hybrid density functional^{46,47} and the 6-311G(d,p) triple- ζ basis set³³ when studying aluminum content. This model chemistry has proven effective at capturing acid-base energetics in zeolites.⁴⁸ In contrast, when studying ion exchange, we used a mixed basis set: the SDD basis set⁴⁹ for alkali atoms and 6-311G(d,p) for all other elements. This mixed basis set approach is necessitated by the fact that 6-311G(d,p) is not available for the heavier alkali metals Rb or Cs. We determined the error from this mixed basis set by computing BF_3 sorption energies at isolated basic sites in 12T/92T clusters with Li, Na, or K comparing results from SDD and 6-311G(d,p) descriptions of the alkali metals. As shown in Table 1, the SDD basis set slightly underestimates sorption energies by 1–4% (maximum error 3.8 kJ/mol) with error decreasing as metal size increases. This mixed basis set approach thus appears to be an effective way for treating heavier metals in zeolites.

For the low level of theory, we applied the universal force field (UFF)⁵⁰ with hydrogen, oxygen, nitrogen, and boron atom types specified as H, O_3_z, N_3, and B_2, respectively.⁵⁰ The use of B3LYP/6-311G(d,p)//UFF with these ONIOM cluster sizes has previously been shown to give converged energies for proton transfer in zeolites.³¹ For each system with Na atoms in the outer layer, we fixed outer-layer Na positions since UFF was not found to reproduce Na distributions in zeolites satisfactorily. However, all inner-layer Na atoms were allowed to relax fully. Geometry optimizations were performed with no symmetry constraints and using the quadratic coupling method,^{51,52} which couples forces between ONIOM layers in a numerically

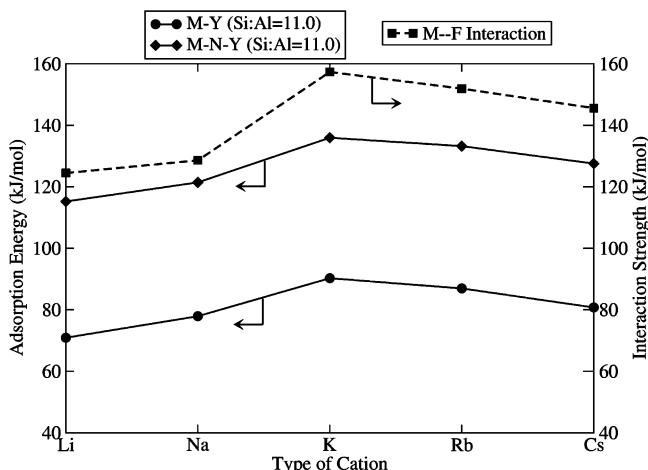


Figure 2. Base strength in standard (M–Y) and nitrated (M–N–Y) zeolites (Si:Al = 11) probed by BF₃ sorption energies as a function of ion exchange.

TABLE 2: Selected Binding Distances (Å) from BF₃ Sorption in M–Y and M–N–Y Zeolites

	M–Y		M–N–Y	
	O(1)–B	F–M	N–B	F–M
Li	1.62	1.92	1.64	1.87
Na	1.62	2.33	1.65	2.27
K	1.61	2.56	1.64	2.55
Rb	1.61	2.68	1.64	2.67
Cs	1.61	2.84	1.63	2.84

stable fashion. All calculations were performed using Gaussian Development Version (release D.02)⁵³ on Linux workstations.

To understand trends in sorption energies, we computed atomic charges using two methods. When studying the effect of aluminum content on basicity with 6-311G(d,p), we computed charges fitted to the electrostatic potential (ESP charges) at points selected by the Merz–Singh–Kollman scheme.^{54,55} Unfortunately, using this approach with the mixed basis set treatment of ion exchange presented numerical difficulties. As such, in this case, we used Mulliken population analysis for computing atomic charges. Although ESP charges offer a more robust representation of charge distributions (less basis set dependence), Mulliken charges offer qualitative trends for a given basis set.

3. Results and Discussion

Here, we present our predictions on the effect of aluminum content and ion exchange on the base strength of faujasites (M–Y) and nitrated faujasites (M–N–Y) by comparing sorption energies of probe molecules BF₃ and BH₃. Following our earlier study,⁸ we begin by investigating the effect of ion exchange with BF₃ as the probe; we then consider BH₃ as a better probe using this to study ion exchange first and Al content second.

3.1. BF₃ as Probe Molecule. We begin by reporting calculated sorption energies of BF₃ in M–Y and M–N–Y zeolites for alkali metals M = Li, Na, K, Rb, and Cs. Sorption energies of BF₃ are shown in Figure 2 for M–Y and M–N–Y, while binding distances and Mulliken charges on selected atoms are given in Tables 2 and 3. Figure 2 shows considerable increases in base strength upon nitridation for all alkali metals from about 80 kJ/mol in M–Y to 120 kJ/mol in M–N–Y. This increase is consistent with our earlier study of basicity in silica sodalite, where BF₃ binding increases from about 50 to 80 kJ/mol upon

TABLE 3: Mulliken Charges (au) on Selected Atoms from BF₃ Sorption in M–Y and M–N–Y Zeolites

	O(1) (N) ^a	B ^a	F ^a	M ^a
Li	−0.861 (−0.943)	0.698 (0.687)	−0.362 (−0.380)	0.474 (0.479)
Na	−0.860 (−0.944)	0.685 (0.676)	−0.346 (−0.366)	0.625 (0.632)
K	−0.854 (−0.909)	0.676 (0.664)	−0.357 (−0.372)	0.813 (0.818)
Rb	−0.852 (−0.930)	0.679 (0.659)	−0.351 (−0.362)	0.834 (0.841)
Cs	−0.849 (−0.920)	0.685 (0.647)	−0.342 (−0.354)	0.870 (0.876)

^a The values in parentheses are for sorption in nitrated zeolites.

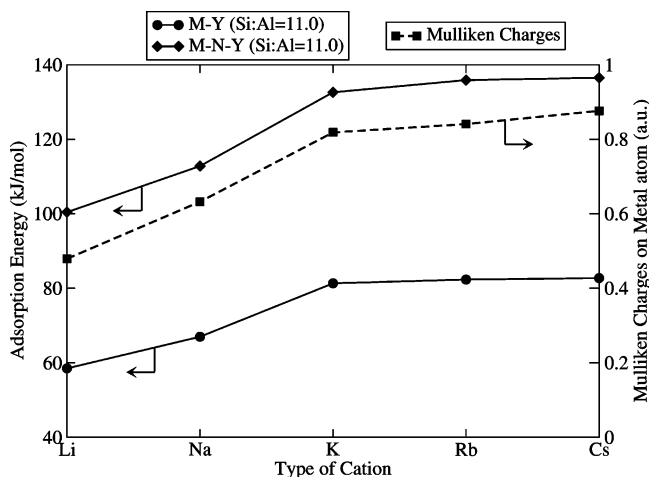


Figure 3. Base strength in standard (M–Y) and nitrated (M–N–Y) zeolites (Si:Al = 11) probed by BH₃ sorption energies as a function of ion exchange.

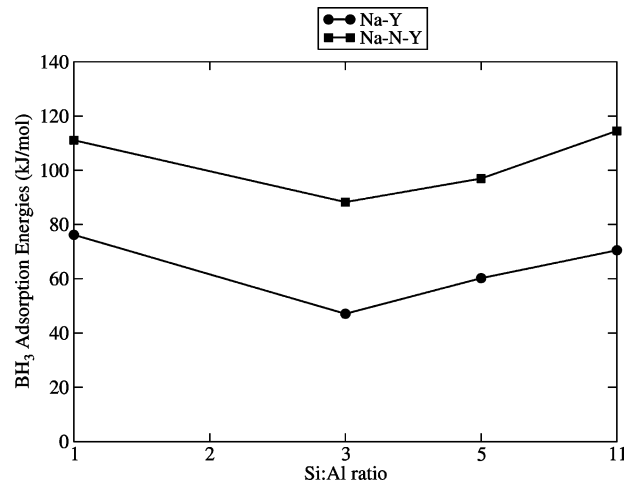


Figure 4. Base strength in Na–Y and nitrated Na–N–Y zeolites probed by BH₃ sorption energies as a function of aluminum content.

nitridation.⁸ Figure 2 also shows that sorption energies follow the trend Li < Na < K > Rb > Cs for both M–Y and M–N–Y zeolites. In contrast, experiments find that basicity increases monotonically in the order Li < Na < K < Rb < Cs.^{23,24} To address this discrepancy, we analyze binding distances and atomic charges in Tables 2 and 3.

Table 2 indicates that the B–O/N binding distance decreases slightly as the size of the alkali metal increases from Li to Cs suggesting that the fundamental Lewis acid–base interaction strengthens slightly. Table 3 shows increased negative charge from O to N in all cases studied consistent with stronger sorption in nitrated zeolites as seen in Figure 2. Ion exchange from Li to Cs shows increasing positive charge on the alkali atom, while fluorine charges exhibit a nonmonotonic trend mirroring the sorption energies in Figure 2. These fluorine charges suggest

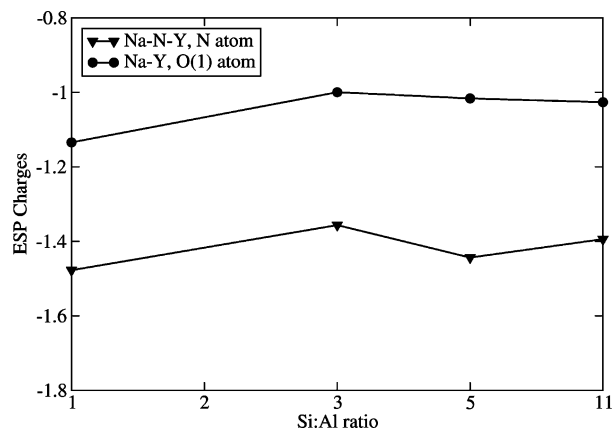


Figure 5. Electrostatic potential (ESP) charges on O/N atoms in Na–Y and nitrated Na–N–Y zeolites, respectively, as a function of aluminum content.

that the sorption energies in Figure 2 may be influenced by metal–fluorine Coulomb interactions.

To test this idea, we calculated metal–fluorine Coulomb interactions, $Q_M Q_F / R_{MF}$, using metal–fluorine distances (R_{MF}) from Table 2 and charges (Q_M , Q_F) from Table 3. In this analysis of BF_3 –M interactions, we consider only the closest metal–fluorine contact, whose distance is given in Table 2. As seen in Figure 2 (dashed line), these Coulomb interactions exhibit the same trend as the BF_3 sorption energies indicating that competing metal–fluorine interactions obfuscate inherent trends in base strength upon ion exchange. The presence of metal–fluorine electrostatic interactions between the adsorbed molecule with fluorine and the zeolitic Na ion has also been shown previously by Mellot and Cheetham,⁵⁶ who performed canonical Monte Carlo simulations on the adsorption of fluorinated molecules in zeolites. To eliminate such interactions, we have pursued BH_3 as a probe in our work below.

3.2. BH_3 as Probe Molecule: Effect of Ion Exchange. The effect of ion exchange on BH_3 sorption energies is plotted in Figure 3 showing a monotonic increase in base strength from Li to Cs. Figure 3 shows the same ~ 40 kJ/mol boost in sorption energy upon nitridation as seen in Figure 2. Furthermore, Figure 3 shows that BH_3 sorption energies increase only mildly from K to Cs (by ~ 5 kJ/mol). This is explained by the Mulliken charges on alkali atoms (dashed line in Figure 3), which exhibit the same plateau from K to Cs. This plateau in alkali charges indicates that K, Rb, and Cs donate approximately the same amount of charge density to the framework producing basic sites of roughly the same strength. The same trend was also observed for Si:Al = 5.0. We determined this by randomly substituting Al (following Löwenstein’s rule) and placing a cation nearby. This structure was then fully optimized, and probe molecule adsorption calculations were performed. Because ion exchange with Rb and Cs can be expensive, the results in Figure 3 suggest that K–N–Y may be optimal for base catalytic applications balancing base strength and catalyst cost.

3.3. BH_3 as Probe Molecule: Effect of Aluminum Content. A conventional wisdom in zeolite science is that increasing aluminum content (decreasing Si:Al ratio) increases base strength by adding negative charge density to framework oxygens.²² To test this notion in Na–Y and nitrated Na–N–Y zeolites, we computed BH_3 sorption energies as a function of aluminum content shown in Figure 4. This shows the now standard 35–40 kJ/mol boost in sorption energy upon nitridation. Figure 4 also shows that BH_3 sorption energies decrease with increasing Si:Al ratio from 1 to 3 beyond which base strength was found to increase again. The initial regime ($1 < \text{Si:Al} < 3$) is consistent with the conventional understanding discussed above, while the latter regime ($\text{Si:Al} > 3$) involves the surprising prediction that base strength can be relatively high for high-silica zeolites. In particular, Figure 4 predicts that BH_3 sorption in Na–N–Y (Si:Al = 11, one Al atom) is nearly as strong as in (Si:Al = 1, six Al atoms). Although these results

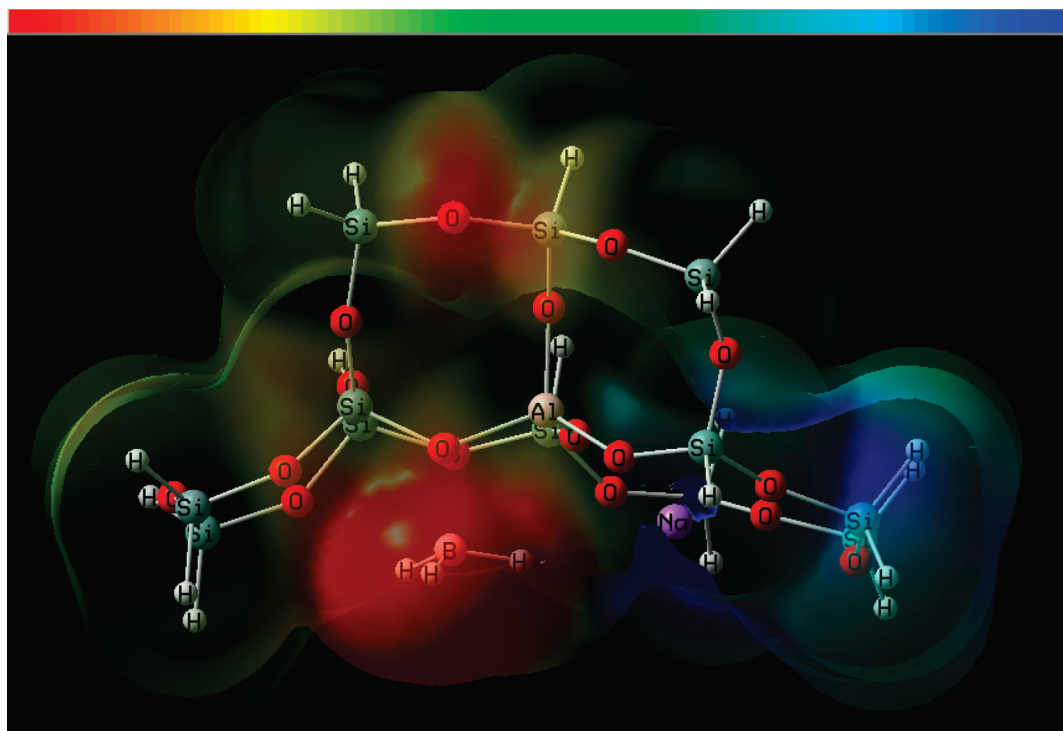


Figure 6. Electrostatic potential map for Si:Al = 11.0 (one Al atom), charge scale on top with red being most negative and blue being most positive.

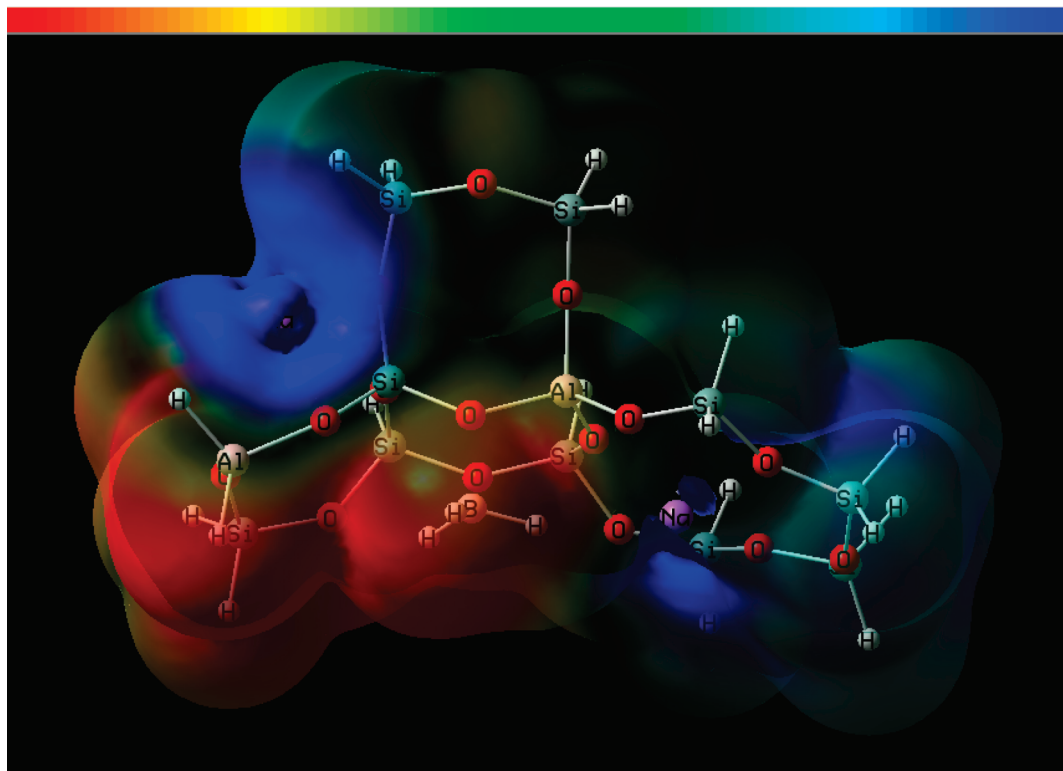


Figure 7. Electrostatic potential map for Si:Al = 5.0 (two Al atoms), charge scale on top with red being most negative and blue being most positive.

seem to contradict experimental findings,²² measurements of FAU-type base strengths have been performed on the standard Si:Al ratios of 1.2 (Na-X) and 2.4 (Na-Y). Our calculations prompt new experiments on base strengths of dealuminated Y zeolites with Si:Al ratios much above 3. Because high-silica zeolites are typically more stable to the kinds of hydrothermal treatments used to regenerate catalysts, these results suggest that K-N-Y (Si:Al = 11) may optimize the balance between base strength and catalyst cost/stability.

To understand these computational findings, we computed charges fitted to electrostatic potential (ESP) values at points selected by the Merz-Singh-Kollman scheme.^{54,55} As seen in Figure 5, these ESP charges show substantially more negative charge on nitrogen than on oxygen for each Si:Al ratio in qualitative agreement with the Mulliken charges in Table 3. Figure 5 also shows nonmonotonic trends in N/O charges as a function of Si:Al ratio. For $1 < \text{Si:Al} < 3$, N/O charges become less negative with increasing Si:Al as expected by conventional wisdom. However, for $\text{Si:Al} > 3$, these charges become more strongly negative for reasons we do not presently understand.

To go beyond the point-charge analysis in Figure 5, we computed electrostatic potential maps for Si:Al = 11 and 5 (one and two Al atoms in the quantum cluster); these are shown in Figures 6 and 7, respectively. As seen from Figures 6 and 7, the additional framework electron density from increased Al content is localized around the bridging atoms (O or NH) near the substituted Al atom and is not delocalized throughout the framework. This localized effect suggests that, for a single adsorbed BH_3 molecule, increasing Al content increases the number of strong basic sites but not the strength of already strong base sites. As such, we find the nonmonotonic trend to be essentially flat.

4. Conclusions

We have applied quantum chemistry to model base strengths of standard and nitrogen-substituted (nitrided) FAU-type zeo-

lites, denoted M-Y and M-N-Y, respectively. We calculated sorption energies of probe molecules BF_3 and BH_3 using density functional theory with mixed basis sets applied to embedded clusters. Mixed basis sets were required because the 6-311G(d,p) basis set is not available for all alkali metals, namely, Rb and Cs. BH_3 was found to be a better probe of base strength because it does not introduce competing metal-fluorine interactions that obfuscate trends. In all cases, the base strengths of M-N-Y were found to exceed those of the corresponding M-Y zeolites by roughly 40 kJ/mol, where M = Li, Na, K, Rb, or Cs charge-compensating cations. We have found for Si:Al = 11 that BH_3 sorption energies vary in the order $\text{Li} < \text{Na} < \text{K} \sim \text{Rb} \sim \text{Cs}$. Sorption energy and hence base strength was found to decrease with increasing Si:Al ratio from 1 to 3 beyond which base strength was found to increase again. The initial regime ($1 < \text{Si:Al} < 3$) is consistent with the prevailing understanding that base strength increases with Al content, while the latter regime ($\text{Si:Al} > 3$) involves the surprising prediction that base strength can be relatively high for the more stable, high-silica zeolites. Taken together, these results suggest that K-N-Y (Si:Al = 11) optimizes the balance of catalyst activity, stability, and cost. Our calculations prompt new experiments on base strength in standard and nitrided zeolites especially for Na-Y and K-Y with Si:Al ratios above 3.

Acknowledgment. We thank Dr. K. Hammond, Dr. G. Tompsett, and Prof. J. T. Fermann at UMass Amherst, Dr. T. Vreven at UMass Worcester, and Dr. F. Clemente at Gaussian, Inc., for their expertise. We also thank Prof. C. Grey and F. Dogan at Stony Brook University for stimulating discussions and collaborations on nitrided zeolites. We are grateful for generous funding from the National Science Foundation (CBET-0553577 and CBET-0932777) and the Department of Energy (DEFG027ER15918).

References and Notes

- (1) Auerbach, S. M.; Carrado, K. A.; Dutta, P. K. *Handbook of Zeolite Science and Technology*; Marcel Dekker, Inc.: New York, 2003.
- (2) Huber, G. W.; Iborra, S.; Corma, A. *Chem. Rev.* **2006**, *106*, 4044.
- (3) Hattori, H. *Chem. Rev.* **1995**, *95*, 537.
- (4) Ono, Y.; Baba, T. *Catal. Today* **1997**, *38*, 321.
- (5) Weitkamp, J.; Hunger, M.; Rymasa, U. *Microporous Mesoporous Mater.* **2001**, *48*, 255.
- (6) Kerr, G. T.; Shipman, G. F. *J. Phys. Chem.* **1968**, *72*, 3071.
- (7) Guillou, N.; Gao, Q.; Forster, P. M.; Chang, J. S.; Nogues, M.; Park, S. E.; Ferey, G.; Cheetham, A. K. *Angew. Chem., Int. Ed.* **2001**, *40*, 2831.
- (8) Astala, R.; Auerbach, S. M. *J. Am. Chem. Soc.* **2004**, *126*, 1843.
- (9) Ernst, S.; Hartmann, M.; Sauerbeck, S.; Bongers, T. *Appl. Catal., A* **2000**, *200*, 117.
- (10) Narasimharao, K.; Hartmann, M.; Thiel, H. H.; Ernst, S. *Microporous Mesoporous Mater.* **2006**, *90*, 377.
- (11) Hammond, K. D.; Auerbach, S. M. *Modeling the Structure and Spectroscopy of Alkaline Zeolites. In Silica and Silicates in Modern Catalysis*; Kerala: Research Signpost ed.; Halasz, I., Ed.; 2010, p. 29.
- (12) Dogan, F.; Hammond, K. D.; Tompsett, G. A.; Huo, H.; Conner, W. C.; Auerbach, S. M.; Grey, C. P. *J. Am. Chem. Soc.* **2009**, *131*, 11062.
- (13) Fink, P.; Datka, J. *J. Chem. Soc., Faraday Trans. 1* **1989**, *85*, 3079.
- (14) Guo, J.; Han, A.-J.; Yu, H.; Dong, J.-P.; He, H.; Long, Y.-C. *Microporous Mesoporous Mater.* **2006**, *94*, 166.
- (15) Hammond, K. D.; Dogan, F.; Tompsett, G. A.; Agarwal, V.; W. Curtis, C., Jr.; Grey, C. P.; Auerbach, S. M. *J. Am. Chem. Soc.* **2008**, *130*, 14912.
- (16) Hammond, K. D.; Gharibeh, M.; Tompsett, G. A.; Dogan, F.; Brown, A. V.; Grey, C. P.; Auerbach, S. M.; Conner, W. C. *Chem. Mater.* **2010**, *22*, 130.
- (17) Han, A. J.; He, H. Y.; Guo, J.; Yu, H.; Huang, Y. F.; Long, Y. C. *Microporous Mesoporous Mater.* **2005**, *79*, 177.
- (18) Han, A. J.; Zeng, Y.; Guo, J.; Huang, Y. F.; He, H. Y.; Long, Y. C. *Chin. J. Chem.* **2005**, *23*, 413.
- (19) Srasra, M.; Poncelet, G.; Grange, P.; Delsarte, S. Nitrided Ultrastable Zeolite Y: Identification and Quantification of Incorporated Nitrogen Species and their Influence on the Basic Catalytic Activity. In *Sieves: From Basic Research to Industrial Applications, Pts A and B*; 3rd Conference of the Federation-of-European-Zeolite-Association, Prague, Czech Republic, Aug 23-29, 2005; Cejka, J., Zilkova, N., Nachtigall, P., Eds.; Studies in Surface Science and Catalysis; Elsevier Science, BV: Amsterdam, The Netherlands, 2005; Vol. 40, pp 1811-1818.
- (20) Agarwal, V.; Huber, G. W.; Conner, W. C.; Auerbach, S. M. *J. Catal.* **2010**, *269*, 53.
- (21) Agarwal, V.; Huber, G. W.; Conner, W. C.; Auerbach, S. M. *J. Catal.* **2010**, *270*, 249.
- (22) Barthomeuf, D. *Catal. Rev.—Sci. Eng.* **1996**, *38*, 521.
- (23) Barthomeuf, D. *J. Phys. Chem.* **1984**, *88*, 42.
- (24) Barthomeuf, D.; Coudurier, G.; Viedrine, J. C. *Mater. Chem. Phys.* **1988**, *18*, 553.
- (25) Huang, M.; Adnot, A.; Kaliaguine, S. *J. Catal.* **1992**, *137*, 322.
- (26) Huang, M.; Adnot, A.; Kaliaguine, S. *J. Am. Chem. Soc.* **1992**, *114*, 10005.
- (27) Huang, M.; Kaliaguine, S. *J. Chem. Soc., Faraday Trans.* **1992**, *88*, 751.
- (28) Xie, J. H.; Huang, M. M.; Kaliaguine, S. *React. Kinet. Catal. Lett.* **1996**, *58*, 217.
- (29) Xie, J. H.; Huang, M. M.; Kaliaguine, S. *Appl. Surf. Sci.* **1997**, *115*, 157.
- (30) Okamoto, Y.; Ogawa, M.; Maezawa, A.; Imanaka, T. *J. Catal.* **1988**, *112*, 427.
- (31) Fermann, J. T.; Moniz, T.; Kiowski, O.; McIntire, T. J.; Auerbach, S. M.; Vreven, T.; Frisch, M. J. *J. Chem. Theory Comput.* **2005**, *1*, 1232.
- (32) Mignon, P.; Geerlings, P.; Schoonheydt, R. *J. Phys. Chem. B* **2006**, *110*, 24947.
- (33) Krishnan, R.; Binkley, J. S.; Seeger, R.; Pople, J. A. *J. Chem. Phys.* **1980**, *72*, 650.
- (34) Lavalley, J. C.; Lamotte, J.; Travert, A.; Czyzniewska, J.; Ziolek, M. *J. Chem. Soc., Faraday Trans.* **1998**, *94*, 331.
- (35) Heidler, R.; Janssens, G.; Mortier, W. J.; Schoonheydt, R. A. *J. Phys. Chem.* **1996**, *100*, 19728.
- (36) Mishin, I. V.; Brueva, T. R.; Kapustin, G. I. *Adsorption-J. Int. Adsorpt. Soc.* **2005**, *11*, 415.
- (37) Tsutsumi, K.; Mitani, Y.; Takahashi, H. *Bull. Chem. Soc. Jpn.* **1983**, *56*, 1912.
- (38) Auroux, A.; Viedrine, J. C. Microcalorimetric characterization of acidity and basicity of various metallic oxide. In *Studies in Surface Science Catalysis*; Imelik, B., Naccache, C., Coudurier, G., Ben Taarit, Y., Viedrine, J. C., Eds.; Elsevier: Amsterdam, 1985; Vol. 20, p 311.
- (39) Hriljac, J. A.; Eddy, M. M.; Cheetham, A. K.; Donohue, J. A.; Ray, G. J. *J. Solid State Chem.* **1993**, *106*, 66.
- (40) Dapprich, S.; Komaromi, I.; Byun, K. S.; Morokuma, K.; Frisch, M. J. *J. Mol. Struct.: THEOCHEM* **1999**, *462*, 1.
- (41) Morokuma, K.; Dapprich, S.; Komaromi, I.; Froese, R. D.; Holthausen, M.; Musae, D. G.; Byun, S.; Khoroshun, S. *Abstr. Pap. Am. Chem. Soc.* **1997**, *214*, 74.
- (42) Vreven, T.; Morokuma, K.; Farkas, O.; Schlegel, H. B.; Frisch, M. J. *J. Comput. Chem.* **2003**, *24*, 760.
- (43) Buttefey, S.; Boutin, A.; Mellot-Draznieks, C.; Fuchs, A. H. *J. Phys. Chem. B* **2001**, *105*, 9569.
- (44) Jaramillo, E.; Auerbach, S. M. *J. Phys. Chem. B* **1999**, *103*, 9589.
- (45) Morokuma, K. *Bull. Korean Chem. Soc.* **2003**, *24*, 797.
- (46) Becke, A. D. *J. Chem. Phys.* **1993**, *98*, 5648.
- (47) Lee, C. T.; Yang, W. T.; Parr, R. G. *Phys. Rev. B* **1988**, *37*, 785.
- (48) Fermann, J. T.; Blanco, C.; Auerbach, S. *J. Chem. Phys.* **2000**, *112*, 6779.
- (49) Fuentealba, P.; Preuss, H.; Stoll, H.; Vonszentpaly, L. *Chem. Phys. Lett.* **1982**, *89*, 418.
- (50) Rappe, A. K.; Casewit, C. J.; Colwell, K. S.; Goddard, W. A.; Skiff, W. M. *J. Am. Chem. Soc.* **1992**, *114*, 10024.
- (51) Vreven, T.; Byun, K. S.; Komaromi, I.; Dapprich, S.; Montgomery, J. A.; Morokuma, K.; Frisch, M. J. *J. Chem. Theory Comput.* **2006**, *2*, 815.
- (52) Vreven, T.; Frisch, M. J.; Kudin, K. N.; Schlegel, H. B.; Morokuma, K. *Mol. Phys.* **2006**, *104*, 701.
- (53) Frisch, M. J.; Trucks, G. W.; Schlegel, H. B.; Scuseria, G. E.; Robb, M. A.; Cheeseman, J. R.; J. A. Montgomery, J.; Vreven, T.; Kudin, K. N.; Burant, J. C.; Millam, J. M.; Iyengar, S. S.; Tomasi, J.; Barone, V.; Mennucci, B.; Cossi, M.; Scalmani, G.; Rega, N.; Petersson, G. A.; Nakatsuji, H.; Hada, M.; Ehara, M.; Toyota, K.; Fukuda, R.; Hasegawa, J.; Ishida, M.; Nakajima, T.; Honda, Y.; Kitao, O.; Nakai, H.; Klene, M.; Li, X.; Knox, J. E.; Hratchian, H. P.; Cross, J. B.; Bakken, V.; Adamo, C.; Jaramillo, J.; Gomperts, R.; Stratmann, R. E.; Yazyev, O.; Austin, A. J.; Cammi, R.; Pomelli, C.; Ochterski, J. W.; Ayala, P. Y.; Morokuma, K.; Voth, G. A.; Salvador, P.; Dannenberg, J. J.; Zakrzewski, V. G.; Dapprich, S.; Daniels, A. D.; Strain, M. C.; Farkas, O.; Malick, D. K.; Rabuck, A. D.; Raghavachari, K.; Foresman, J. B.; Ortiz, J. V.; Cui, Q.; Baboul, A. G.; Clifford, S.; Cioslowski, J.; Stefanov, B. B.; Liu, G.; Liashenko, A.; Piskorz, P.; Komaromi, I.; Martin, R. L.; Fox, D. J.; Keith, T.; Al-Laham, M. A.; Peng, C. Y.; Nanayakkara, A.; Challacombe, M.; Gill, P. M. W.; Johnson, B.; Chen, W.; Wong, M. W.; Gonzalez, C.; Pople, J. A. Gaussian Development Version, Revision D.02.
- (54) Besler, B. H.; Merz, K. M.; Kollman, P. A. *J. Comput. Chem.* **1990**, *11*, 431.
- (55) Singh, U. C.; Kollman, P. A. *J. Comput. Chem.* **1984**, *5*, 129.
- (56) Mellot, C. F.; Cheetham, A. K. *J. Phys. Chem. B* **1999**, *103*, 3864.